Loss-Minimization-Based Charging Strategy for Lithium-Ion Battery

Zheng Chen, *Senior Member, IEEE*, Bing Xia, *Student Member, IEEE*, Chunting Chris Mi, *Fellow, IEEE*, and Rui Xiong, *Member, IEEE*

***Abstract*—In this paper, an optimal charging strategy for lithium-ion batteries is proposed to minimize charging loss. To reach this target, a one-RC electric model is employed to model the loss for the battery, and an efficiency map is measured for the charger, considering different charging currents and voltages. A dynamic programming algorithm is applied to determine the optimal charging current profiles for minimizing the losses of the battery and the charger separately and collectively. Experiment results prove that the proposed method is more efficient compared with a constant-current charging method without influencing the charging time.**

***Index Terms*—Battery charger, dynamic programming (DP), lithium-ion battery, loss minimization, state of charge (SoC).**

I. Introduction

THE development of electric vehicles (EVs) and plug-in hybrid EVs (PHEVs) has been greatly promoted due to limited fossil fuel and environmental issues. The demand for rechargeable batteries, which serve as the key energy storage element in EVs and PHEVs, is expanding correspondingly. Among all the types of rechargeable batteries, lithium-ion batteries dominate the market because of its high-power density, high-energy density, and long life cycle and they are free of memory effect [1], [2]. Abundant research has been carried out for lithium-ion batteries, including battery status estimation [2], which mainly consists of battery state of charge (SoC) [3], state of health (SoH) [4], and state of function (SoF) estimation, and battery charge strategy research [5]. The traditional charging scheme for lithium-ion batteries is the constant-current–constant-voltage method. This method consists of two stages, i.e., a constant-current (CC) charging stage and a constant-voltage (CV) stage. During the CC mode, a constant charging current is applied to the terminal of the battery until its terminal voltage reaches a predetermined maximum value. Then, the charging process is transferred into CV charging mode. During this mode, the battery terminal voltage remains unchanged, and the charging current will gradually decrease until a cutoff current threshold is reached. This charging method is easy to implement due to its simplicity. However, it does not consider the charging loss, and the charging efficiency may not be high. Since the battery internal resistance varies with battery SoC, we believed that the varied charging current can possibly decrease the charging loss without shortening the battery life, thereby improving charging efficiency.

Many charging strategies have been introduced to improve the charging efficiency, shorten the charging time, or extend battery life. In [6], an ant-algorithm-based charging pattern strategy is proposed to reduce charging time and extend battery life. It takes advantage of the positive feedback and distributed computation of the ant-colony system. However, the optimal charging solution takes relatively long time to obtain, and it does not have a physical model to work with. In [7], a fuzzy controlled active SoC controller is applied to substitute the CV charging mode. However, the implementation of these techniques is too complex. In [8] and [9], pulse current charging is proposed with respect to electrochemistry reaction, which allows lithium ions to diffuse more evenly throughout the battery and thus alleviate polarization. In this scenario, the rising time, pulse amplitude, and frequency should be well tuned to have the best performance, and they are different among various kinds of batteries. In [10], temperature is considered as a state, and by manipulating weight terms in cost functions, optimal charging profiles could be determined with different purposes, including final cell temperature, final SoC, and energy loss. By rearranging the charging scheme, this method could remove the warm-up stage, which is necessary in cold start, thus saving energy usage. However, it requires a more accurate estimation at the end stage where current is largest, which might lead to safety concerns if full charge is required. In [11], an optimal charging strategy is proposed based on nonlinear model predictive control techniques to charge the lithium-ion battery in a fast way, while guaranteeing safety throughout the battery life. It concerns the safety, temperature increment, and mechanical stress of the battery; however, it does not take into account the charger losses to optimize the total charging efficiency. In [12], a model predictive control framework is introduced to optimize the charging current, considering the battery temperature. A genetic algorithm is employed to optimize the charging current profile under multiple objectives. In

Manuscript received October 23, 2014; revised January 12, 2015; accepted March 9, 2015. Date of publication March 30, 2015; date of current version September 16, 2015. Paper 2014-TSC-0779, presented at the 2014 IEEE Energy Conversion Congress and Exposition, Pittsburgh, PA, USA, September 20–24, and approved for publication in the IEEE TRANSACTIONS ON INDUSTRY APPLICATIONS by the Transportation Systems Committee of the IEEE Industry Applications Society.

Z. Chen is with the Faculty of Transportation Engineering, Kunming University of Science and Technology, Kunming 650500, China (e-mail: botaoc@gmail.com).

B. Xia and C. C. Mi are with the Department of Electrical and Computer Engineering, University of Michigan–Dearborn, Dearborn, MI 48128 USA (e-mail: xiabing@umich.edu; chrismi@umich.edu).

R. Xiong is with the School of Mechanical Engineering, Beijing Institute of Technology, Beijing 100081, China (e-mail: rxiong@bit.edu.cn).

Color versions of one or more of the figures in this paper are available online at http://ieeexplore.ieee.org.

Digital Object Identifier 10.1109/TIA.2015.2417118

[13], a dynamic optimization method to maximize the energy storage for the lithium-ion battery is presented. However, it does not detail the analysis of obtaining the charging current profile. In [14], a multiobjective optimal charging problem for two types of lithium-ion batteries is formulated to optimally trade off the conflict between charging time and energy loss. In [15], two varied charged current profiles are employed to illustrate better charging efficiency and capacity retention. In [16], the optimal charging current for the lithium-ion battery is traded off between cycle life, time-to-charge, energy losses, and temperature rise.

Until now, there has been little work done to improve the overall efficiency, including both battery efficiency and charger efficiency. For a lithium-ion battery, an equivalent electric circuit model [3] is easy to build, which can simulate the battery performance with high precision. In [17], an improved model for lithium-ion batteries is proposed, which varies cell resistance and electrode overpotential with respect to temperature. These models can guarantee the effectiveness of simulating the battery static and dynamic performances. Given the battery model, the available charging time, the initial SoC, and the target SoC, the charging strategy can be optimized to decrease the charging loss. For a battery charger, its efficiency changes with different voltage and current levels and can be easily measured. Hence, the optimal charging scheme, which minimizes the power loss of the charger, can be also calculated. Finally, an overall charging loss minimization can be achieved by considering the loss of the battery and the charger together. This is the main motivation of this paper.

To realize the mentioned target, a battery model should be built first to obtain the relationship between charging loss and charging current. In this paper, an equivalent circuit model [4], [18], which has been widely used for battery state estimations, is introduced to describe the battery static and dynamic performances. Based on the built model, the charging loss can be easily calculated with respect to battery current. Then, dynamic programming (DP) [19], [20] is applied to find the optimal charging current profile. DP is a method that converts complex problems into multiple subproblems. The cost of each subproblem is computed, recorded, and looked up when the same step is encountered again in computation. Finally, DP selects the optimal solution by comparing all existing steps. The advantage of this method is that it can find the optimal solution even for a nonlinear system without too much calculation labor. Moreover, an optimal charging current profile for the charger is achieved by DP through relating charger loss with output voltage and current. Finally, an overall optimal charging scheme is obtained by considering both losses. Experiment results prove that the proposed strategy can dramatically improve charging efficiency.

II. Charging Loss Modeling

To minimize the charging loss, loss models for the battery and the charger should be properly built. Here, an equivalent circuit model is introduced to analyze the charging loss for the battery, an efficiency map is measured for the charger at different output voltage and current levels, and experiment results validate the effectiveness of the models.

Fig. 1. Tested pouch cell.

TABLE I
Specifications of the Battery Cell

Material	Lithium-ion polymer
Capacity (Nominal at C/2)	40Ah
Nominal voltage	3.7V
Lower limit voltage	2.7V
Upper limit voltage	4.2V

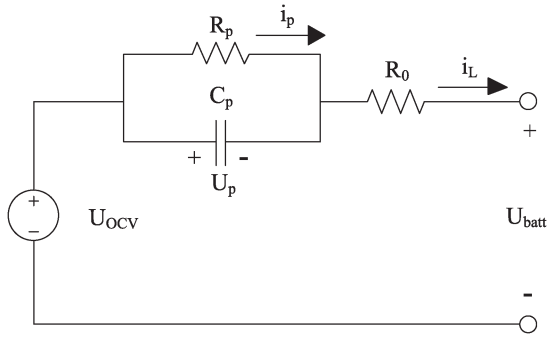

Fig. 2. Equivalent circuit model for lithium-ion battery.

A. Lithium-Ion Battery Cell Modeling

A lithium-ion polymer pouch cell, as shown in Fig. 1, is tested using Arbin battery test equipment at normal room temperature. The basic specifications of the battery pouch cell are listed in Table I. The rated capacity of the battery is 40 ampere-hour (Ah), and its nominal voltage is 3.7 V.

The equivalent circuit model [3], [21] for the battery is shown in Fig. 2, which consists of an open-circuit voltage (OCV) source $U_{\rm ocv}$; a polarized resistor R_p, which is in parallel with a capacitor C_p; and a resistor R_0. $U_{\rm ocv}$ characterizes the nonlinear relationship between OCV with battery SoC. R_p and C_p network models the transient response due to the polarization and diffusion effect, and R_0 describes the immediate voltage drop after current excitation.

To build the battery model, some particular experiments need to be conducted to capture the battery static and dynamic characteristics, which includes static capacity test, OCV test, hybrid pulse power characterization (HPPC) test, and drive cycle test [3]. The whole test process for modeling the battery

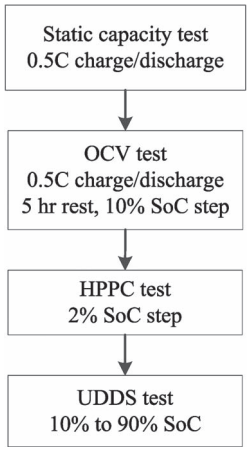

Fig. 3. Test procedures for battery modeling.

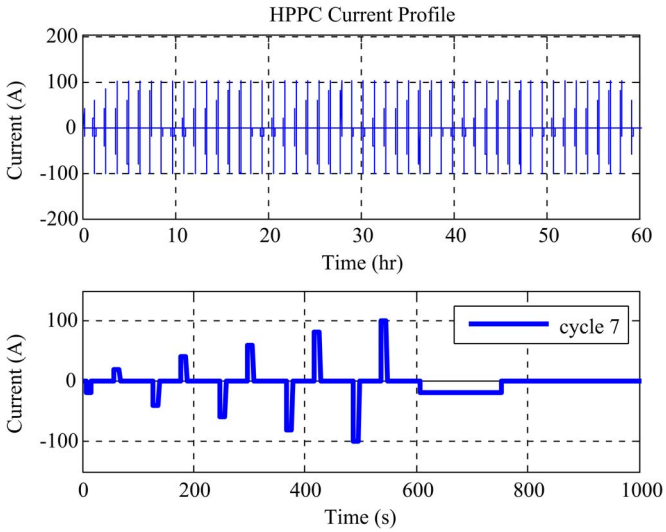

Fig. 4. HPPC test.

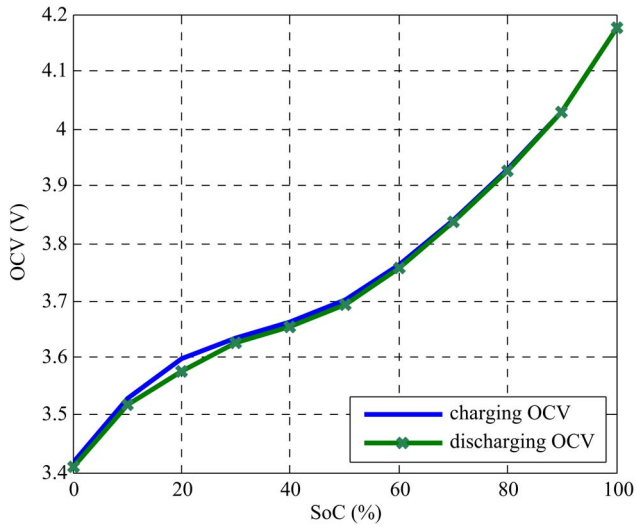

Fig. 5. OCV with respect to SoC.

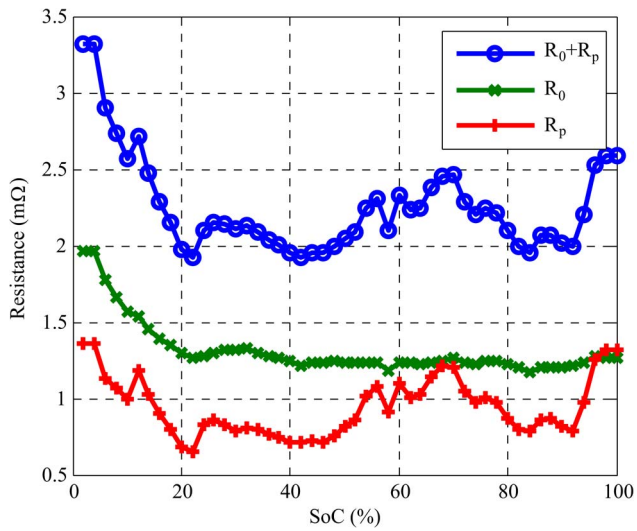

Fig. 6. R_0 and R_p dependence on SoC.

and validating the built model is shown in Fig. 3. The function of the static capacity test is to test the battery capacity with recommended charging current, i.e., 0.5 C, where C is the value of the current with which the battery can be discharged for 1 h. The OCV test is to obtain the battery static voltage with different SoC levels when the battery is not connected to the circuit. The OCV tests are recorded with a step of 10% SoC. As shown in Fig. 4, the HPPC test is applied with a step of 2% SoC to characterize the battery dynamic performance. The main purpose of the drive cycle test is to compare the actual battery terminal voltage with the model output to verify its effectiveness. In this paper, urban dynamometer driving schedule (UDDS) tests are applied to verify the model.

The battery OCV curve is shown in Fig. 5, from which we can see the charging OCV and discharging OCV range from 3.40 to 4.18 V, and there exists a hysteresis between them. R_0, R_p, and their sum value are shown in Fig. 6. Their sum value varies from 3.4 to 1.9 mΩ when SoC ranges from 0 to 1. The variation of C_p with SoC is shown in Fig. 7, and it varies from 35230F to 18610F. Ten consecutive UDDS drive cycle tests are applied to verify the correctness of the model output. Fig. 8 compares the measured battery terminal voltage and model output and shows that the difference is less than 40 mV. Thus, it proves that the model can simulate the battery performance with acceptable accuracy.

B. Lithium-Ion Battery Loss

Given the built model, the power loss of the two energy dissipation elements, i.e., R_0 and R_p, can be calculated accordingly as

$$P_{\text{loss,cell}} = i_p^2 R_p + i_L^2 R_0 \tag{1}$$

where i_p is the current of R_p, i_L denotes the current flowing through R_0, and $P_{\text{loss,cell}}$ is the power loss of the cell. Since R_0 and R_p both vary with battery SoC, we can get the total energy loss during the charge process, i.e.,

$$E_{\text{cell,loss}} = \int_0^{t_f} \left[i_p^2(t) R_p(\text{SoC}) + i_L^2(t) R_0(\text{SoC}) \right] dt \tag{2}$$

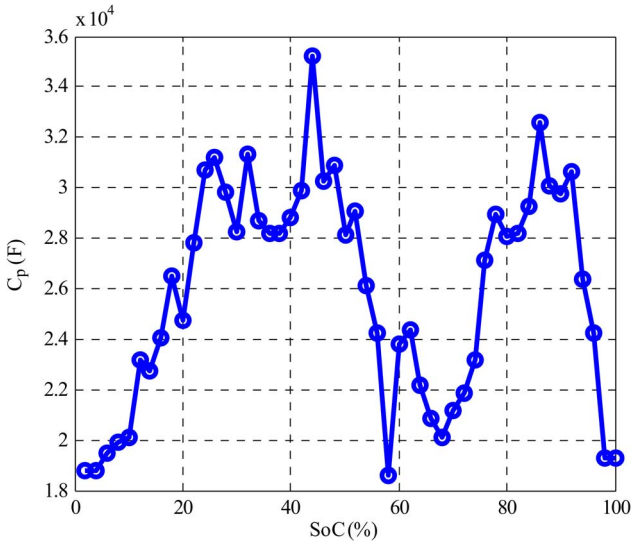

Fig. 7. C_p variation with different SoC levels.

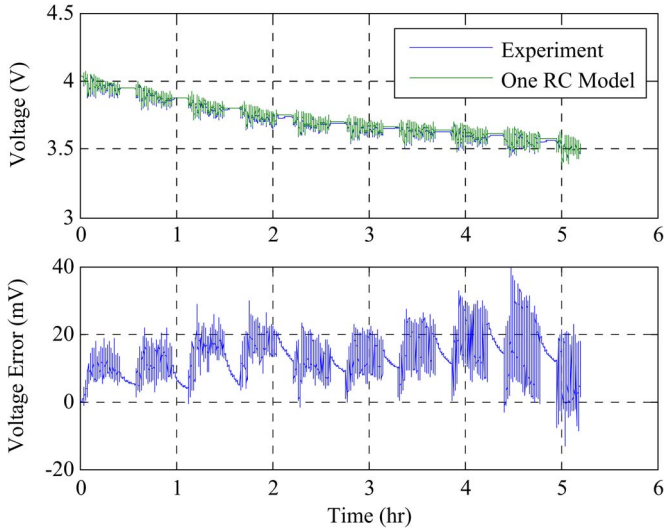

Fig. 8. Model validation with UDDS drive cycle tests.

where t_f is the total charging time, and $E_{\text{cell,loss}}$ is the energy loss of the cell. During the charging process, SoC variation can be calculated as

$$\text{SoC}_{t_f} = \text{SoC}_0 - \frac{1}{C_b}\int_0^{t_f} i_L dt. \tag{3}$$

Based on (2) and (3), the battery charging losses can be calculated when charging the battery with a CC.

Fig. 9 shows the calculated losses and measured losses when the battery is charged using a CC of 0.1–0.5 C. It shows that the calculated losses occupy around 80% of the experimental losses. The remaining part of the losses may come from heat generation from electrochemical reaction or temperature change, which is beyond the scope of the electric model. In this paper, we only focus on the resistance heat loss of the battery when it is charged.

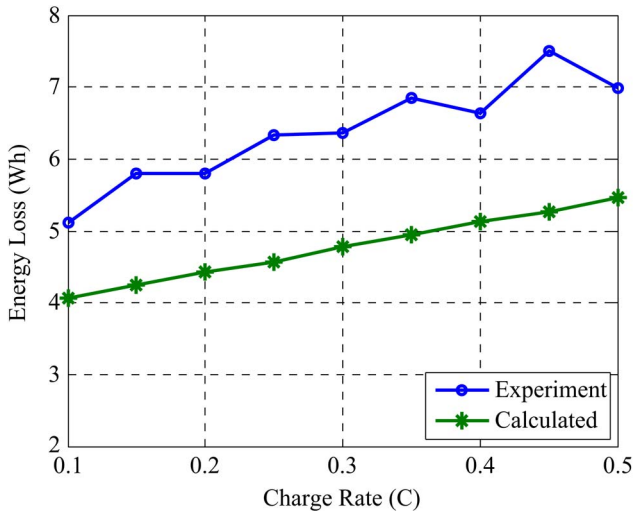

Fig. 9. Calculated and empirical losses.

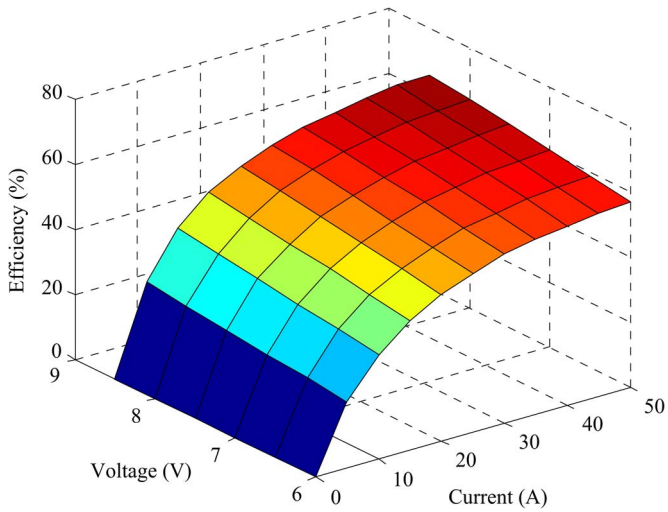

Fig. 10. Efficiency map for the charger.

C. Charger Loss

A Xantrex XDC 10-600 power source is controlled as a battery charger with a maximum voltage of 10 V. Its efficiency is measured with a WT1800 precision power analyzer when the output voltage ranges from 6 to 8.5 V at a step of 0.5 V and the output current ranges from 0 to 50 A at a step of 5 A, as shown in Fig. 10. Due to the voltage limit of the power source and the current limit of the power analyzer, two cells are connected in series as a module in the experiment setup.

During the charging process, the charger efficiency changes due to variations in output voltage and current. Its terminal voltage in the charging mode is calculated according to an electric equivalent model, and the charger power loss is calculated, as presented in (4) and (5), respectively. Thus,

$$U_{\text{batt}} = U_{\text{ocv}}(\text{SoC}) + [R_0(\text{SoC}) + R_p(\text{SoC})]\, I \tag{4}$$

$$P_{\text{loss,charger}} = U_{\text{batt}} I \left(\frac{1}{\eta(U_{\text{batt}}, I)} - 1\right) \tag{5}$$

TABLE II
VALIDATION FOR CHARGER LOSS MODELING

Charge rate (C)	Experiment (Wh)	Simulation (Wh)	Error (Wh)	Error (%)
0.25	480.98	502.17	21.19	4.41
0.50	298.09	309.67	11.58	3.88
0.75	241.86	249.55	7.70	3.18
1.00	200.13	198.52	1.61	0.80

where η is the efficiency of the charger, and $P_{\text{loss,charger}}$ is the power loss of the charger.

Table II shows the comparison of the modeled loss of the charger with experiment results at different charging rates. It shows that the loss model for the charger can estimate the loss of the charger within 4.41% error.

III. DP AND APPLICATION

DP is considered as a cost-effective method in the energy loss calculation. DP expresses complex practical problems as multistage decision processes. It builds loss matrices that save the data, which are most likely to be frequently used in future calculation to save computation time [22].

A. Minimization of Battery Loss

The charging process can be regarded as battery SoC changes from an initial state $\text{SoC}_{\min}$ to the final state $\text{SoC}_{\max}$ within the given charging time t_{charge}. There are many possible paths, i.e., charging profiles, although the start point and the end point are determined. The goal of this paper is to use DP to find an optimal charging current profile with which the energy loss can be minimized.

The charging energy loss from SoC_i to SoC_{i+1} can be expressed in a discrete form as

$$E_i^{\text{loss,cell}} = \left[i_{p,i}^2 R_p(\text{SoC}_i) + i_{L,i}^2 R_L(\text{SoC}_i)\right](t_{i+1} - t_i). \quad (6)$$

Here, since C_p is large enough and there is only a small difference between i_L and i_P when charging the battery, we assume that i_L is equal to i_P to simplify the problem without sacrificing the validity. Hence, we can obtain

$$E_i^{\text{loss,cell}} = i_{L,i}^2 \left[R_p(\text{SoC}_i) + R_L(\text{SoC}_i)\right](t_{i+1} - t_i). \quad (7)$$

To realize DP, some constraints should be properly considered, and the optimization problem is subject to the constraints, i.e.,

$$I_0 = \frac{[(\text{SoC}_{\max} - \text{SoC}_{\min})C_b]}{t_{\text{charge}}} \quad (8)$$

$$I_{\max} = 2I_0 \quad (9)$$

where t_{charge} is the charging time in hours, I_0 is the current value if the battery cell is charged in CC mode during the whole charging process, C_b denotes the battery-rated capacity, $I_{\max}$ is the maximum charging current, and we define it as two times of I_0. The minimum current $I_{\min}$ is set to zero. To solve the problem with acceptable accuracy and without too much calculation labor, the current step value I_{step} is defined as

$$I_{\text{step}} = \frac{I_0}{50} \quad (10)$$

$$I = k \cdot I_{\text{step}}, \quad k = 0, 1, 2, \ldots, 50. \quad (11)$$

From (11), there are, in total, 51 selections for current commands during the calculation. The task of DP is to find a sequence of optimal current commands from them. To realize DP, a loss matrix with respect to different SoC and charging current levels should be constructed to build the cost-to-go matrix [20], [23]. After the loss matrix is constructed, DP will choose the best path to the current state as follows:

$$\begin{aligned} &\min\_\text{cost}_{\text{soc}_{i-1}} + \text{loss}_{\text{soc}_{i-1}} < \min\_\text{cost}_{\text{soc}_i} \\ &\min\_\text{cost}_{\text{soc}_i} = \min\_\text{cost}_{\text{soc}_{i-1}} + \text{loss}_{\text{soc}_{i-1}} \end{aligned} \quad (12)$$

where $\min\_\text{cost}_{\text{soc}_i}$ is the minimum cost at SoC_i, and $\text{loss}_{\text{soc}_{i-1}}$ is the loss at SoC_{i-1}.

By comparing the cost of all the paths that pass the current state, this algorithm ensures that at time t, SoC_i is reached with minimum energy loss, and the cost is stored as $\min\_\text{cost}_{\text{soc}_i}$. The same calculation will be carried out repeatedly until $\text{SoC}_{\max}$ and t_{charge} are reached. As such, the final result will be the minimized energy loss in the charging process. Based on this calculation, the optimal current profile can be searched in a backward way.

Fig. 11 shows the optimal charging current profile based on the proposed method and the CC method, both in the time domain and the SoC domain. The total charging time is 1 h. We can see that using the CC method, the current is 32 A, whereas using the proposed method, the current varies from 26.2 to 35.2 A. Fig. 12 shows the charging current variation and resistance variation with battery SoC. It can be seen that, within the 0%–80% SoC range, DP assigned the current in the pattern that the charging current is relatively higher where the resistance is lower, the charging current is relatively lower where the resistance is higher, and the average charging current is maintained the same as that of the CC method. This way, the charging losses can be decreased. To some extent, it can explain why the proposed method can improve the charging efficiency.

B. Minimization of Charger Loss

During the charging process, the loss of the charger is dependent on cell SoC and charging current. The energy loss from SoC_i to SoC_{i+1} can be expressed in a discrete form as

$$\begin{cases} U_{\text{batt},i} = U_{\text{ocv}}(\text{SoC}_i) + \left[R_0(\text{SoC}_i) + R_p(\text{SoC}_i)\right] I_i \\ E_i^{\text{loss,charger}} = U_{\text{batt},i} I_i \left[1/\eta_i(U_{\text{batt},i}, I_i) - 1\right](t_{i+1} - t). \end{cases} \quad (13)$$

To easily compare the results, the constraints for DP are shown in (14), and the current step is set to 1 A. Thus,

$$\begin{cases} I_{\min} = 0 \\ I_{\max} = 50 \\ \text{SoC}_{\min} = 0 \\ \text{SoC}_{\max} = 80. \end{cases} \quad (14)$$

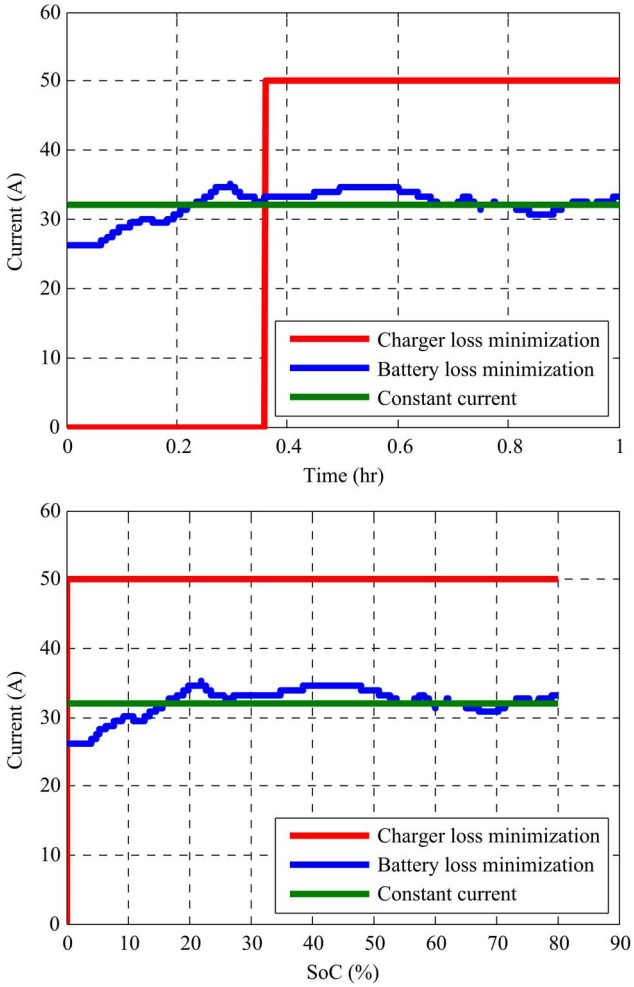

Fig. 11. Optimal charging current.

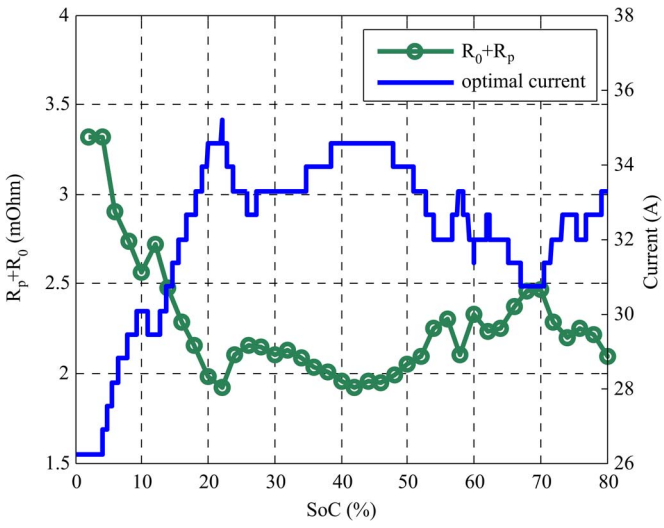

Fig. 12. Cell optimal current profile and resistance of the battery cell.

Here, we simply set the battery initial SoC and ending charger SoC to 0% and 80%, respectively. The maximum charging current is 50 A, and the total charging duration is set to 1–3 h to compare the performances of the proposed algorithm.

DP can also be applied to find the optimal charging scheme when only the charger loss is taken into consideration. Fig. 11 shows the optimal current profile for charger loss minimization when charging for 1 h compared with the CC method. In Fig. 10, the efficiency of the power source depends on the combination of voltage and current. The maximum efficiency is achieved when both voltage and current are maximized within their ranges. As a result, an optimal charging profile can be found when the voltage and current are both maximized. Thus, the charging current is set to the maximum allowable charging current, and the terminal voltage can be maximized according to (4).

It is interesting to note that the current is zero before the maximum current charging. It indicates that even for a longer period of charging time, DP will still find the same optimal charging schemes that remain zero current at the beginning and use maximum current to charge from 0% to 80% SoC. This is because the charger has a higher efficiency when the output current is higher, which makes DP always search for the highest efficient operating point. In addition, it also implies that the optimal charging current is not unique in this problem. The charging process can start at the beginning, and the current remains zero after 80% charged. This is due to the fact that DP can always guarantee one optimal solution; however, it cannot find all optimal solutions if they are not unique.

Based on [24], the charging scheme can be improved further if the maximum current charging time is distributed among charging duration in pulse charging form instead of CC charging. This can be done by adding a penalty function into DP that takes the battery health into account. In this paper, we only focus on the charging efficiency, and the health penalty will be studied in our future work.

IV. Experiment Validation and Discussion

Validation experiments are performed by applying both the optimal current profiles and the normal CC profile. Moreover, for easy comparison, the battery cell and pack are both discharged with 1-C current at room temperature. The energy loss difference in the two charging scenarios is the energy saved by applying the optimal current profile. The energy loss can be calculated as

$$E_{\text{loss}} = \int_{t_1}^{t_2} V(t)I(t)dt - \int_{t_3}^{t_4} V(t)I(t)dt \tag{15}$$

where t_1, t_2, t_3, t_4 are the beginning time and ending time for both the charging process and the discharging process, respectively. The beginning and ending values of the SOC can be easily set up. In this paper, we only assign the beginning SoC as 0% and target charging SoC as 80% to compare the improvements.

A. Cell Loss Minimization

Fig. 13 shows the optimal charging current series for 0%–80% SoC with difference charging time. The charging time ranges from 1 to 3 h with a step of 0.5 h. The charging current

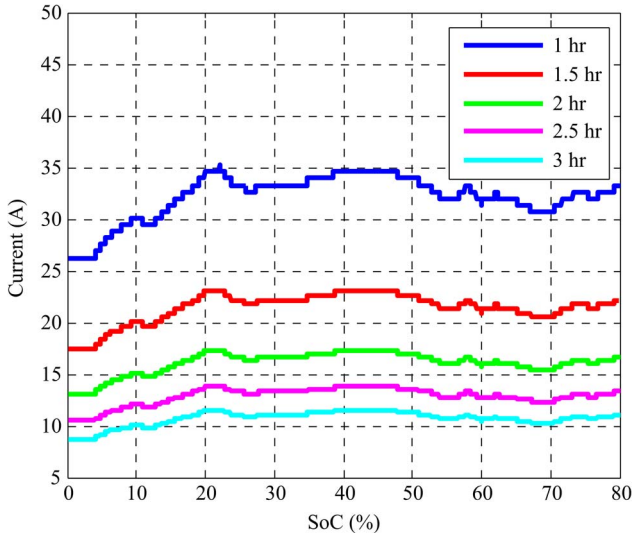

Fig. 13. Cell optimal current profile for 1–3 h.

TABLE III
COMPARISON OF CC AND BATTERY LOSS MINIMIZATION CHARGING

Time (hr)	CC loss (Wh)	Optimal loss (Wh)	Energy saved (Wh)	Energy saved (%)
1.0	7.75	7.60	0.15	1.85
1.5	7.40	7.09	0.32	4.28
2.0	6.67	6.53	0.15	2.24
2.5	6.96	6.81	0.15	2.18
3.0	6.64	6.32	0.32	4.81

commands with different SoC levels look similar. However, when the charging time increases, the charging current profile will become flatter. This is because the charging loss is proportional to charging time and resistance but quadratic to charging current.

Table III compares the charging loss with different charging current levels. It can save 1.85%, 4.28%, 2.24%, 2.18%, and 4.81% when charging time changes from 1 to 3 h. It shows that the proposed method is effective in decreasing the charging loss, thus improving the charging efficiency.

B. Charger Loss Minimization

The optimal current for charger loss minimization is shown in Fig. 11. As discussed in the previous section, the optimal currents keep unchanged as the charging time varies. The energy savings are mainly induced by the difference in efficiency during the charging process. Table IV compares the charging loss with different charging time. The result shows that this method could effectively decrease the loss of the charger.

C. Overall Loss Minimization

It needs to note that both of these two optimal current profiles are the results for local optimization, i.e., battery loss minimization and charger loss minimization, respectively. They are not necessarily the global optimization for the whole charging process.

TABLE IV
COMPARISON OF CC AND CHARGER LOSS MINIMIZATION CHARGING

Time (hr)	CC loss (Wh)	Optimal loss (Wh)	Energy saved (Wh)	Energy saved (%)
1.0	174.32	148.56	25.77	14.78
1.5	221.82	148.56	73.26	33.03
2.0	272.18	148.56	123.62	45.42
2.5	320.71	148.56	172.16	56.68
3.0	380.67	148.56	231.82	60.94

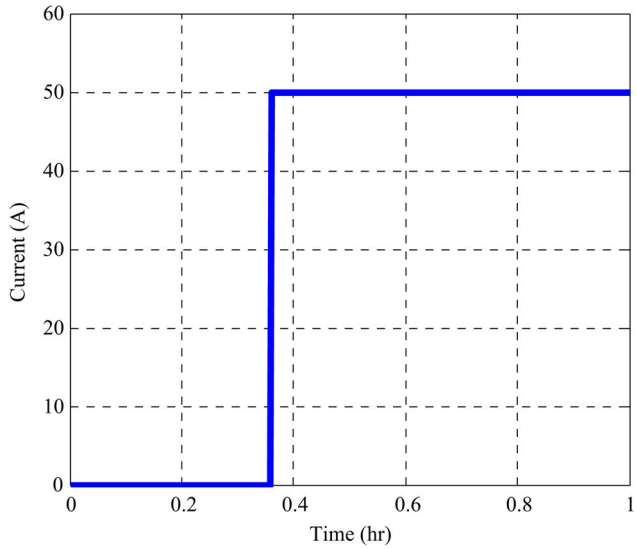

Fig. 14. Overall optimal current for 1-h charging.

Based on their step loss expressions, an overall loss minimization can be achieved by adding them at each step in DP. Since the overall loss involves two parts, i.e., battery loss and charger loss, we can infer that when the charger loss dominates, the overall optimal current should look closer to the charger optimal current, and vice versa.

In the overall optimal current calculation, the battery module consists of two 40-Ah pouch cell in series connection. Fig. 14 shows the overall optimal current profile for the 1-h charging process, which is the same as the current profile when optimizing the charging efficiency only. This is due to the fact that the losses from the two battery cells are negligible when compared with that from the charger.

As shown in Fig. 13, when the charging time increases, the average charging current becomes lower. From (7), a lower charging current leads to a lower loss for the battery, and from Fig. 10, a lower average current indicates a higher loss of the charger. From Tables III and IV, we can see that the charger loss is much larger than the battery loss. Therefore, when the charging time is 1 h, the charging scheme for global loss minimization will follow the same trend as that shown in Fig. 11. Table V compares the losses in the CC scheme and the optimal charging scheme. The results show that the optimal scheme can save from 12.37% to 58.12% of energy when the charging time changes between 1–3 h.

Due to the 10-V voltage limitation of the power source and the 50-A current limitation of the power analyzer, experiments

TABLE V
COMPARISON OF CC AND OPTIMAL CHARGING

Time (hr)	CC loss (Wh)		Optimal loss (Wh)		Energy saved (%)
	Cell	Charger	Cell	Charger	
1.0	14.14	174.32	16.59	148.56	12.37
1.5	12.88	221.82	16.59	148.56	29.63
2.0	13.24	272.18	16.59	148.56	42.14
2.5	12.74	320.71	16.59	148.56	50.47
3.0	13.98	380.37	16.59	148.56	58.12

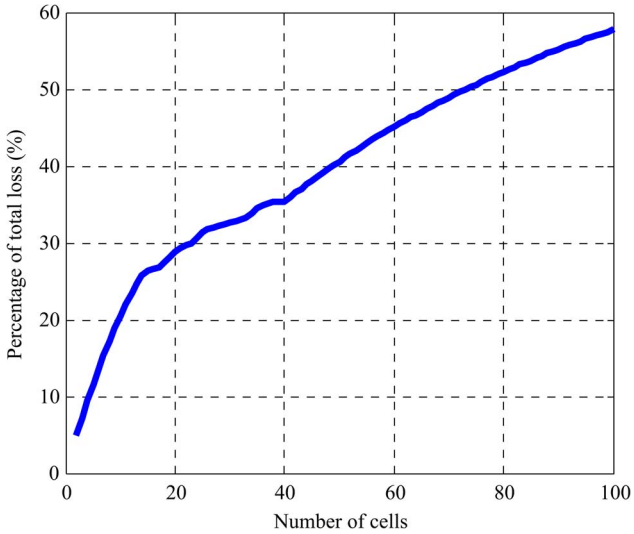

Fig. 15. Increasing portion of cell loss as the number of cell increases.

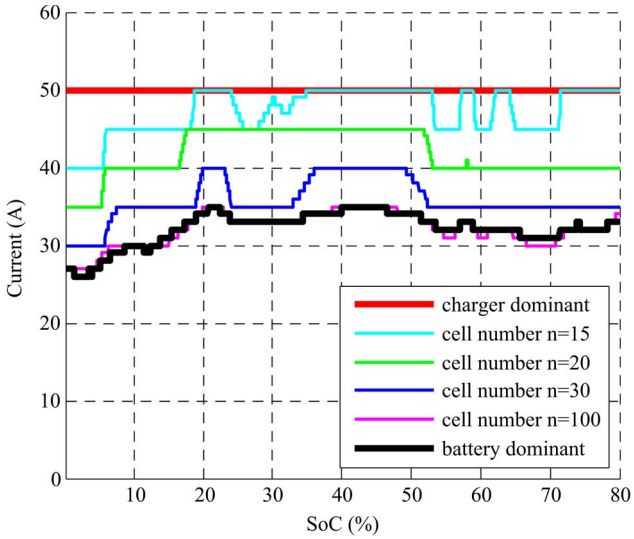

Fig. 16. Two envelopes for global loss minimization.

with more cells were not conducted. However, a simulation is carried out with the assumption that when more cells are connected in series, only the battery loss increases. Fig. 15 shows the battery loss percentage in the whole losses. The result shows that as the number of battery cell increases, the overall optimal current tends to be closer to the battery-only optimal current, as expected. Fig. 16 shows the current profile for different selected numbers of cells in the charging process. Combined with Fig. 15, it can explain that when the battery loss increases, the global optimized currents become closer to optimization curves when considering the batteries only.

The energy savings in Table V largely depend on the wide efficiency band of the power source, which is regarded as the charger in the experiments. In the real case, a commercial charger may not have such a wide efficiency range within its working condition. However, as long as there exist efficiency fluctuations in the charger and SoC-dependent energy loss in the battery, the proposed methodology can still be applied to find the optimal overall charging current to minimize the loss in the whole charging process.

V. CONCLUSION

An optimal charging algorithm for lithium-ion batteries has been proposed to minimize the charging loss of the battery, the charger, and both. DP is applied to find the optimal charging current profile. With knowing the battery beginning SoC, the target SoC, and the charging time, the charging current command can be easily calculated by DP. Compared with the CC charging strategy, the proposed method can effectively decrease the charging loss. Experiment results validated the feasibility of the proposed method for loss minimization in the whole charging process.

Future work can be carried out on pack-level experiments with more cells, improving the performance by evaluating its impact on battery life and adding penalty functions in the DP calculation. In addition, an online improved battery model that considers the influence of battery temperature and aging will be our future work to improve the application of the proposed algorithm.

REFERENCES

[1] C. Mi, M. A. Masrur, and D. W. Gao, *Front Matter*. Hoboken, NJ, USA: Wiley, 2011.
[2] L. Lu, X. Han, J. Li, J. Hua, and M. Ouyang, "A review on the key issues for lithium-ion battery management in electric vehicles," *J. Power Sources*, vol. 226, pp. 272–288, Mar. 2013.
[3] C. Zheng, F. Yuhong, and C. C. Mi, "State of charge estimation of lithium-ion batteries in electric drive vehicles using extended Kalman filtering," *IEEE Trans. Veh. Technol.*, vol. 62, no. 3, pp. 1020–1030, Mar. 2013.
[4] Z. Chen, C. C. Mi, Y. Fu, J.Xu, and X.Gong, "Online battery state of health estimation based on Genetic Algorithm for electric and hybrid vehicle applications," *J. Power Sources*, vol. 240, pp. 184–192, Oct. 2013.
[5] R. D. Anderson, "*Method and system for charging a vehicle high voltage battery*," Google Patents, Sep. 3, 2013.
[6] L. Yi-Hwa, T. Jen-Hao, and L.Yu-Chung, "Search for an optimal rapid charging pattern for lithium-ion batteries using ant colony system algorithm," *IEEE Trans. Ind. Electron.*, vol. 52, no. 5, pp. 1328–1336, Oct. 2005.
[7] H. Guan-Chyun, C.Liang-Rui, and H. Kuo-Shun, "Fuzzy-controlled Li-ion battery charge system with active state-of-charge controller," *IEEE Trans. Ind. Electron.*, vol. 48, pp. 585–593, Jun. 2001.
[8] B. Purushothaman and U.Landau, "Rapid charging of lithium-ion batteries using pulsed currents a theoretical analysis," *J. Electrochem. Soc.*, vol. 153, no. 3, pp. A533–A542, 2006.
[9] L.-R. Chen *et al.*, "Detecting of optimal Li-ion battery charging frequency by using AC impedance technique," in *Proc. IEEE ICIEA*, 2009, pp. 3378–3381.
[10] E. Inoa and J. Wang, "PHEV charging strategies for maximized energy saving," *IEEE Trans. Veh. Technol.*, vol. 60, no. 7, pp. 2978–2986, Sep. 2011.
[11] R. Klein *et al.*, "Optimal charging strategies in lithium-ion battery," in *Proc. ACC*, 2011, pp. 382–387.

[12] Y. Jingyu, X. Guoqing, Q. Huihuan, and X. Yangsheng, "Battery fast charging strategy based on model predictive control," in *Proc. IEEE 72nd VTC-Fall*, 2010, pp. 1–8.
[13] R. Methekar, V. Ramadesigan, R. D. Braatz, and V. R. Subramanian, "Optimum charging profile for lithium-ion batteries to maximize energy storage and utilization," *ECS Trans.*, vol. 25, no. 35, pp. 139–146, 2010.
[14] X. Hu, S. Li, H. Peng, and F. Sun, "Charging time and loss optimization for LiNMC and $LiFePO_4$ batteries based on equivalent circuit models," *J. Power Sources*, vol. 239, pp. 449–457, 2013.
[15] Z. Guo, B. Y. Liaw, X. Qiu, L. Gao, and C. Zhang, "Optimal charging method for lithium ion batteries using a universal voltage protocol accommodating aging," *J. Power Sources*, vol. 274, pp. 957–964, 2015.
[16] B. Pattipati *et al.*, "Integrated battery fuel gauge and optimal charger," in *Proc. IEEE AUTOTESTCON*, 2014, pp. 260–269.
[17] L. W. Juang, P. J. Kollmeyer, T. M. Jahns, and R. D. Lorenz, "Improved modeling of lithium-based batteries using temperature-dependent resistance and overpotential," in *Proc. IEEE ITEC*, 2014, pp. 1–8.
[18] X. Jun *et al.*, "A comparison study of the model based SoC estimation methods for lithium-ion batteries," in *Proc. IEEE VPPC*, 2013, pp. 1–5.
[19] C. Zheng and C. C. Mi, "An adaptive online energy management controller for power-split HEV based on Dynamic Programming and fuzzy logic," in *Proc. IEEE VPPC*, 2009, pp. 335–339.
[20] Z. Chen, C. Mi, J. Xu, X. Gong, and C. You , "Online energy management for a power-split plug-in hybrid electric vehicle based on dynamic programming and neural networks," *IEEE Trans. Veh. Technol.*, vol. 63, no. 4, pp. 1567–1580, May 2013.
[21] Y. Hu, S. Yurkovich, Y. Guezennec, and B. J. Yurkovich, "A technique for dynamic battery model identification in automotive applications using linear parameter varying structures," *Control Eng. Pract.*, vol. 17, pp. 1190–1201, 2009.
[22] D. P. Bertsekas and J. N. Tsitsiklis, "Neuro-dynamic programming: An overview," in *Proc. 34th IEEE Conf. Decision Control*, 1995, pp. 560–564.
[23] Y. L. Murphey *et al.*, "Intelligent Hybrid Vehicle Power Control—Part I: Machine Learning of Optimal Vehicle Power," *IEEE Trans. Veh. Technol.*, vol. 61, no. 1, pp. 3519–3530, Oct. 2012.
[24] R. C. Cope and Y. Podrazhansky, "The art of battery charging," in *Proc. 14th Annu. Battery Conf. Appl. Adv.*, 1999, pp. 233–235.

Zheng Chen (A'10–M'12–SM'14) received the B.S. and M.S. degrees in electrical engineering and the Ph.D. degree in control science engineering from Northwestern Polytechnical University, Xi'an, China, in 2004, 2007, and 2012, respectively.

He is currently a Professor of transportation engineering with Kunming University of Science and Technology, Kunming, China. From 2008 to 2014, he was a Postdoctoral Fellow and a Research Scholar with the University of Michigan–Dearborn, Dearborn, MI, USA. His research interests include battery management systems, battery status estimation, and energy management of hybrid electric vehicles.

Bing Xia (S'13) received the B.S. degree in mechanical engineering from the University of Michigan, Ann Arbor, MI, USA, and the B.S. degree in electrical engineering from Shanghai Jiaotong University, Shanghai, China, in 2012. He is currently working toward the Ph.D. degree in automotive systems engineering in the Department of Electrical and Computer Engineering, University of Michigan–Dearborn, Dearborn, MI.

His research interests focus on batteries, including charging optimization, battery safety, and battery management.

Chunting Chris Mi (S'00–A'01–M'01–SM'03–F'12) received the B.S. and M.S. degrees from Northwestern Polytechnical University, Xi'an, China, and the Ph.D. degree from the University of Toronto, Toronto, ON, Canada, all in electrical engineering.

He is a Professor of electrical and computer engineering and the Director of the Department-of-Energy-funded Graduate Automotive Technology Education Center for Electric Drive Transportation, University of Michigan–Dearborn, Dearborn, MI, USA. Prior to joining the University of Michigan–Dearborn in 2001, he was with General Electric Company, Peterborough, ON. He has conducted extensive research and has published more than 100 journal papers. His research interests include electric drives, power electronics, electric machines, renewable energy systems, and electrical and hybrid vehicles.

Prof. Mi is an Area Editor of the IEEE TRANSACTIONS ON VEHICULAR TECHNOLOGY and an Associate Editor of the IEEE TRANSACTIONS ON POWER ELECTRONICS and the IEEE TRANSACTIONS ON INDUSTRY APPLICATIONS.

Rui Xiong (S'12–M'14) received the M.S. degree in vehicle engineering and the Ph.D. degree in mechanical engineering from Beijing Institute of Technology, Beijing, China, in 2010 and 2014, respectively. From 2012 to 2014, he was a joint Ph.D. student with the U.S. Department of Energy Graduate Automotive Technology Education Center for Electric Drive Transportation, College of Electrical and Computer Science, University of Michigan–Dearborn, Dearborn, MI, USA.

Since 2008, he has been with Beijing Institute of Technology, where he was promoted to Associate Professor in the School of Mechanical Engineering in 2014. He has been invited to speak and serve on panels for several conferences and seminars. He has served as a Reviewer for many journals and conferences. He has more than 40 peer-reviewed articles. His research interests include system identification, state estimation, uncertainty optimal control, and their applications in the areas of electrical and hybrid vehicles and energy storage systems.